

Article

Fabrication of Cost-Effective Dye-Sensitized Solar Cells Using Sheet-Like CoS₂ Films and Phthaloylchitosan-Based Gel-Polymer Electrolyte

Saradh Prasad ^{1,2} , Devaraj Durairaj ^{1,*}, Mohamad Saleh AlSalhi ^{2,3,*} , Jayaraman Theerthagiri ⁴, Prabhakarn Arunachalam ⁵  and Govindarajan Durai ⁴

¹ Department of Electrical and Electronics Engineering, School of Electronics and Electrical Technology (SEET), Kalasalingam Academy of Research and Education (KARE), Krishnankoil, Virudhunagar 626126, Tamil Nadu, India; saradprasad@gmail.com

² Research Chair on Laser Diagnosis of Cancers, Department of Physics and Astronomy, College of Science, King Saud University, 11451 Riyadh, Saudi Arabia

³ Department of Physics and Astronomy, College of Science, King Saud University, 11451 Riyadh, Saudi Arabia

⁴ Centre of Excellence for Energy Research, Sathyabama Institute of Science and Technology, Chennai 600119, India; j.theerthagiri@gmail.com (J.T.); durainayak@gmail.com (G.D.)

⁵ Electrochemistry Research Group, Chemistry Department, College of Science, King Saud University, 11451 Riyadh, Saudi Arabia; parunachalam@ksu.edu.sa

* Correspondence: deva230@yahoo.com (D.D.); malsalhy@gmail.com (M.S.A.); Tel.: +91-984-291-3053 (D.D.); +966-50-510-4815 (M.S.A.)

Received: 25 December 2017; Accepted: 18 January 2018; Published: 24 January 2018

Abstract: Platinum-free counter electrodes (CE) were developed for use in efficient and cost-effective energy conversion devices, such as dye-sensitized solar cells (DSSCs). Electrochemical deposition of CoS₂ on fluorine-doped tin oxide (FTO) formed a hierarchical sheet-like structured CoS₂ thin film. This film was engaged as a cost-effective platinum-free and high-efficiency CE for DSSCs. High stability was achieved using a phthaloylchitosan-based gel-polymer electrolyte as the redox electrolyte. The electrocatalytic performance of the sheet-like CoS₂ film was analyzed by electrochemical impedance spectroscopy and cyclic voltammetry. The film displayed improved electrocatalytic behavior that can be credited to a low charge-transfer resistance at the CE/electrolyte boundary and improved exchange between triiodide and iodide ions. The fabricated DSSCs with a phthaloylchitosan-based gel-polymer electrolyte and sheet-like CoS₂ CE had a power conversion efficiency (PCE, η) of 7.29% with a fill factor (FF) of 0.64, J_{sc} of 17.51 mA/cm², and a V_{oc} of 0.65 V, which was analogous to that of Pt CE ($\eta = 7.82\%$). The high PCE of the sheet-like CoS₂ CE arises from the enhanced FF and J_{sc} , which can be attributed to the abundant active electrocatalytic sites and enhanced interfacial charge-transfer by the well-organized surface structure.

Keywords: CoS₂ film; electrocatalytic activity; counter electrode; dye-sensitized solar cells; gel-polymer electrolyte

1. Introduction

Recently, the emphasis on solar energy has resulted in a paradigm shift in the energy industry, resulting in lower oil prices. Solar energy has recently become a growing part of the energy industry, mostly because of government backing and subsidies, due to its scientific potential and industrial applications as a renewable (at least for next 2 billion years) and sustainable energy source. To compete with other energy sources without subsidies, solar cell technology must be improved in terms of efficiency, cost, large scale production, easy fabrication process, transparency, flexibility,

and environmental friendliness [1–8]. DSSCs have the prospective to fit all of these requirements, and tremendous progress has recently been reported towards these goals. A standard DSSC mimics the photosynthetic process with four major components: the dye as a sensitizer, metal oxide-based semiconductors as the photoanodes, redox electrolyte (usually iodide/triiodide (I^-/I_3^-)), and CE. The CE is a crucial part of DSSCs, as it receives electrons from external loads and catalyzes the reduction of I_3^- to I^- in the electrolyte. An ideal CE would possess a large surface area for electrocatalytic performances, low charge transfer resistance, high stability, superior catalytic reduction properties, and low cost. These properties would decrease the internal series resistance of the device, enabling a high fill factor (FF) of the fabricated device [9–11]. Usually, Pt has been engaged as CE in DSSCs owing to its greater electrocatalytic performance. However, Pt is a noble and scarce metal, and its high cost and disintegration in the redox electrolyte, to produce PtI_4 and H_2PtI_6 , hinder the scaling-up of DSSC production. This has driven several investigators to develop Pt-free electrocatalytic materials with superior electrocatalytic performances concerning the catalytic reduction of I_3^- to I^- ions [12,13].

The redox electrolyte is a key component in DSSCs. The main functions of the redox electrolyte in DSSCs are to regenerate the oxidized sensitizer dye, conduct holes in the DSSCs, and complete the external electrical circuit. The stability of DSSCs is highly dependent on the redox electrolyte and they are generally fabricated with liquid electrolytes (e.g., I^-/I_3^- redox couple) with a high PCE. However, liquid electrolytes have several disadvantages including difficulty in sealing the device, lower stability due to solvent evaporation, solvent leakage, and electrode corrosion [14–20]. To overcome these weaknesses, a popular strategy is to use polymer electrolytes in place of liquid electrolytes.

Numerous Pt-free low cost functional materials have been investigated for their good electrocatalytic activity in DSSCs, including carbon-based materials [21,22], conducting polymers [23], sulfides [24,25], selenides [26], nitrides, and carbides [27,28]. Metal sulfides have fascinated significant consideration due to their distinct physical and chemical properties, high conductivity, high catalytic activity, low toxicity, abundance, and low-cost manufacturing protocol that can be easily modified for multi-purpose applications [29–31]. Recent reports have established that cobalt sulfide-based candidates can be engaged to replace Pt electrocatalysts in DSSCs [32–34]. The electrocatalytic performance of these materials is mostly determined by the nature of the electrocatalytic active sites and the structural morphology of the surface [13,31]. Notably, carbon nanofiber and nano-felt were prepared using electrospinning and found to be low-cost, efficient counter electrodes for DSSCs [35,36].

In this study, a hierarchical structured sheet-like CoS_2 film was fabricated on FTO substrate by electrochemical deposition (ECD) using cyclic voltammetry (CV). The key advantage of the ECD process is that the coating can be deposited over large area using a low-cost manufacturing technique, which can easily be implemented on an industrial scale resulting in good adhesion to the FTO substrates and a uniform coating. In this study, the fabricated solar cells used a polymer gel electrolyte based on phthaloylchitosan. Herein, we have investigated the use of CoS_2 as a cheap electrocatalyst for use in gel-polymer electrolyte-based DSSCs to achieve long-term stability while maintaining a high PCE.

2. Results and Discussion

2.1. XRD Studies

The XRD pattern of the electrochemically deposited CoS_2 thin film on an FTO is shown in Figure 1. Diffraction peaks can be observed at 33.2° , 37.6° , 42.6° , and 57.8° which correspond to the (200), (210), (211), and (311) diffraction planes of cubic CoS_2 . The experimental diffraction peaks match the standard cubic CoS_2 data (PDF card No. 01-077-7559). The other major diffraction peaks are all related to the pure FTO conducting glass substrate, which are in agreement with our previous report [13]. The observed minor diffraction peaks of CoS_2 on FTO substrate might be due to the deposition thickness of CoS_2 film was low content on surface of the FTO glass substrate.

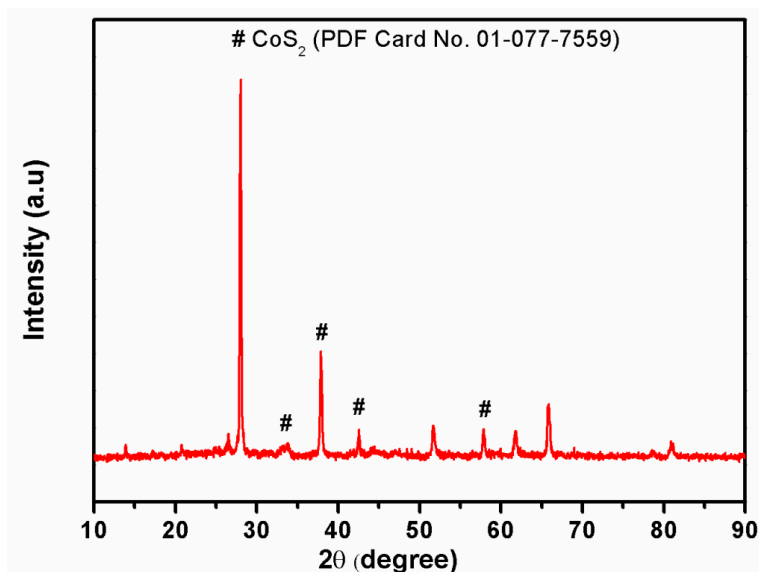
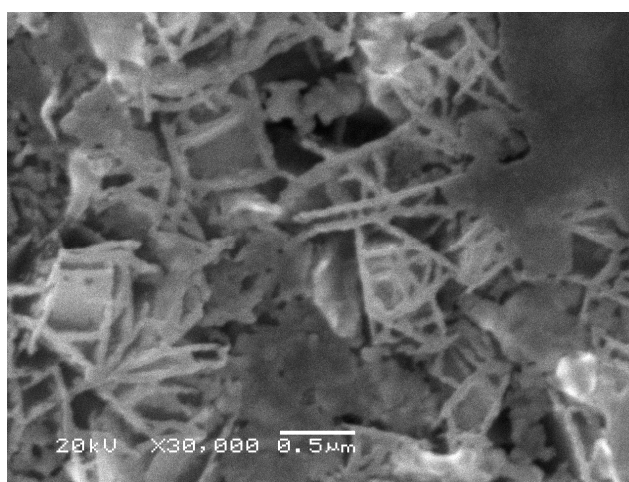


Figure 1. XRD pattern of the as-deposited CoS₂ film.

2.2. Morphology and Elemental Composition Studies

Figure 2a shows the morphological and structural details of the as-deposited CoS₂ film, examined by HRSEM and the corresponding image is shown in Figure 2a. The HRSEM image shows that the pure CoS₂ (Figure 2a) exhibits a sheet-like surface morphology, with some domains comprising a very large quantity of aggregated and irregular particles. The well-organized surface morphology of CoS₂ with firmly stuffed nanocrystals was expected to support efficient charge transport processes at the boundary of the CE surface and gel-polymer redox electrolyte in the prepared DSSCs [9,30]. The HRSEM analysis also revealed that the FTO conducting glass substrate and the as-deposited CoS₂ layers were extremely compatible. Fine adhesion was observed between the FTO glass substrate and the CoS₂ materials and is a significant parameter for defining the stability and PCE of the assembled DSSCs. The energy dispersive X-ray spectroscopy (EDS) elemental analysis of the electrochemically-deposited CoS₂ thin film was performed and shown in Figure 2b, and the pure CoS₂ comprised Co. and S. The additional peaks in Figure 2b likely arise from the FTO [13]. The EDS analysis also revealed the development of the CoS₂ film on the FTO.



(a)

Figure 2. Cont.

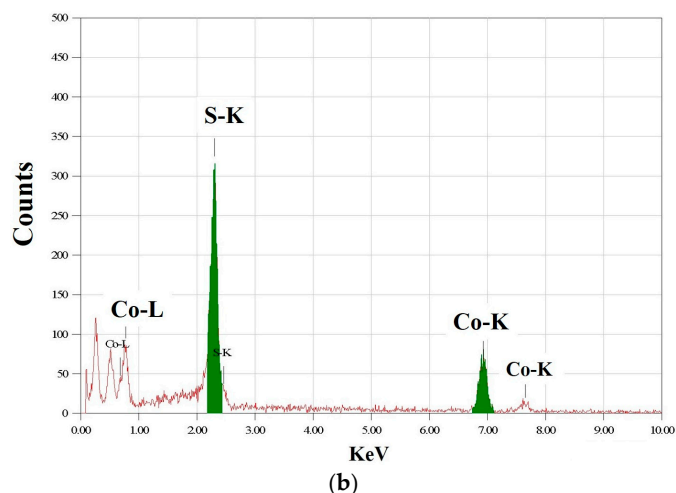


Figure 2. (a) Representative HR-SEM image of the electrodeposited CoS_2 film on FTO; and (b) EDS spectra of the CoS_2 film.

2.3. Electrocatalytic Activity

Electrochemical performance of the as-deposited CoS_2 film and Pt CEs for the catalytic reduction of I_3^- to I^- was investigated by CV using a three-electrode configuration at 150 mV/s. An electrolyte solution containing of 0.01 M I_2 , 0.1 M LiI, and 0.1 M LiClO_4 as a supporting medium in acetonitrile was used. The CVs of the CoS_2 electrocatalyst for the I^-/I_3^- redox species is shown in Figure 3. The redox peaks (Ox-2/Red-2, Ox-1/Red-1) contained two pairs for both the CoS_2 and Pt electrodes. The configuration of right and left redox pairs are shown in Equations (1) and (2).

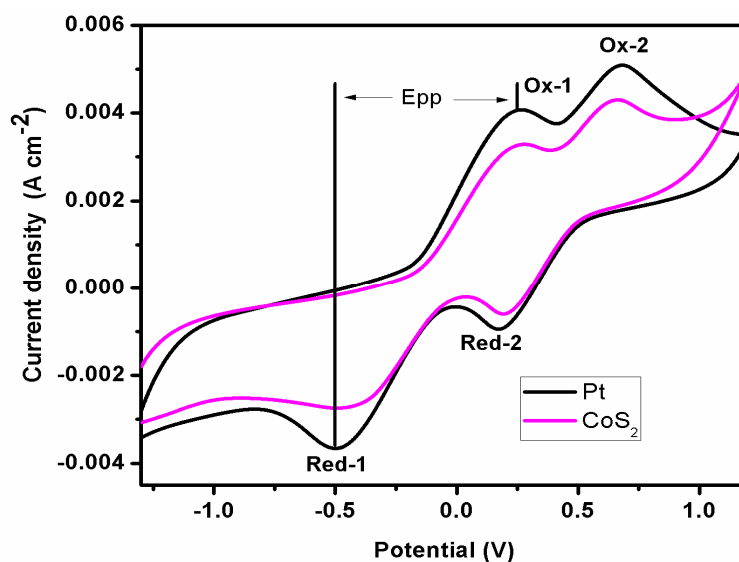


Figure 3. Cyclic voltammograms for the CoS_2 electrocatalyst towards the I^-/I_3^- redox reaction.

As shown in Figure 3, the shape of the CVs of the CoS_2 electrode was similar to that of conventional Pt electrodes under identical operating conditions, which demonstrated similar electrocatalytic behaviors for the I^-/I_3^- redox species.

Electrocatalytic performance of the fabricated CE was investigated by examining the peak-to-peak separation (E_{pp}) and peak current density (PCD or J_{pk}). For efficient electrocatalytic reduction, electrode materials should possess a low E_{pp} and high J_{pk} . Higher J_{pk} values indicate that the reaction rate is faster, whereas a low E_{pp} indicates a smaller over-potential, leading to improved electrocatalytic performance for the reduction of I_3^- [13,31]. The J_{pk} and E_{pp} of the CoS_2 electrode was equivalent to that of the Pt electrode. The experimental CV analysis indicated that the CoS_2 film possesses better performance for the reduction of I_3^- in DSSCs related to the Pt CE.

Figure 4a shows the CV with various scan rates for CoS_2 electrode I^-/I_3^- redox reaction. The J_{pk} tended to increase when the scan rate was increased along with a steady shift of the cathodic and anodic peaks in the direction of positive and negative sides, respectively. This indicates that the inner sites of CoS_2 became more reactive at higher scan rates [10,13]. The linear association between the peak current density and the square root of the scan rates is shown in Figure 4b. The results presented here are consistent with the Langmuir isotherm rule, and the linear correlation indicates that the transport of I^- on the surface of the CoS_2 electrode is influenced by the diffusion control of the redox response [12]. The CV results evidence that the CoS_2 has huge prospective to engage as CEs of DSSCs.

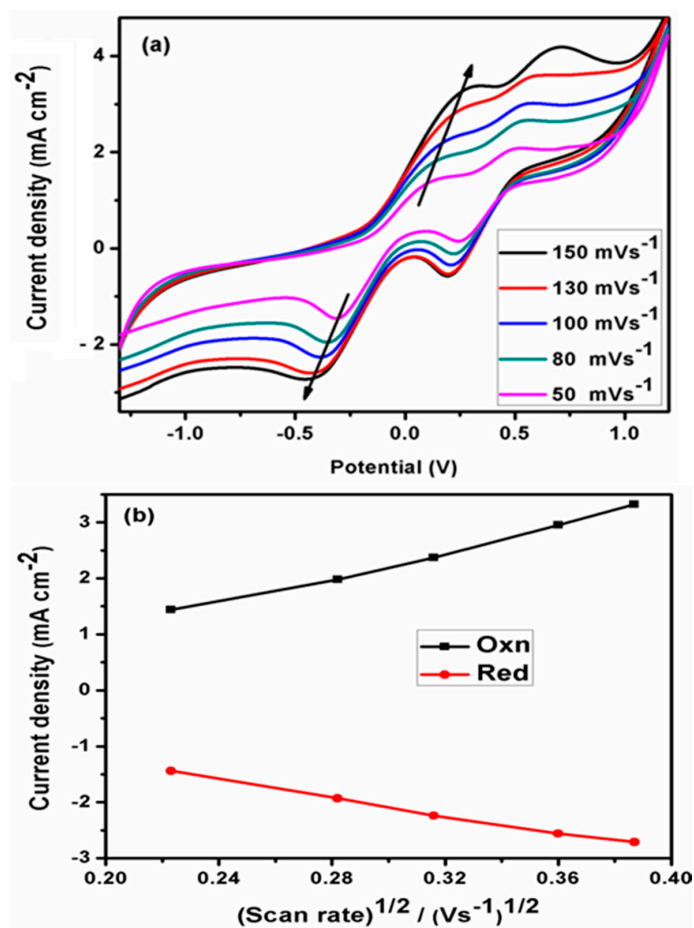


Figure 4. (a) CV curves of the CoS_2 electrode at various scan rates; and (b) linear association between the redox peak current and square root of the scan rate.

2.4. Electrochemical Impedance Spectroscopy (EIS) Studies

Electrocatalytic activity of the as-deposited CoS_2 film was examined by EIS measurement and the resultant Nyquist plot is shown in Figure 5. Charge transfer processes, internal resistance, and the electrocatalytic behavior of the electrodes were effectively determined using the EIS technique [9]. The intercept between the high frequency and real axis (Z' -axis) in the Nyquist plot represents the series

resistance (R_s), and the charge-transfer resistance (R_{ct}) is determined by the area covered under the first semicircle formed at a higher frequency. Moreover, the Nyquist plot contained a second semicircle, which indicates charge recombination between I_3^- ions in the electrolyte and the TiO_2 photoelectrode. Thus, the second semicircle represents the R_{ct} at the interface of the TiO_2 /dye/electrolyte. The focus of the analysis was directed at the first semicircle because it describes the excellent electrocatalytic performance for the I_3^- reduction at the interface of CE/electrolyte. This improved performance was due to the low R_{ct} of the CD, which consequently improved the FF value of the fabricated DSSC device [31]. The R_{ct} value estimated from the Nyquist plot using Z-view software for the CoS_2 electrode was 44.63Ω , comparable to that of the Pt electrode (41.33Ω). This suggests that the CoS_2 film is as efficient as the Pt CE for the reduction of I_3^- to I^- in the fabricated DSSCs. The EIS measurements are in agreement with the CV analysis.

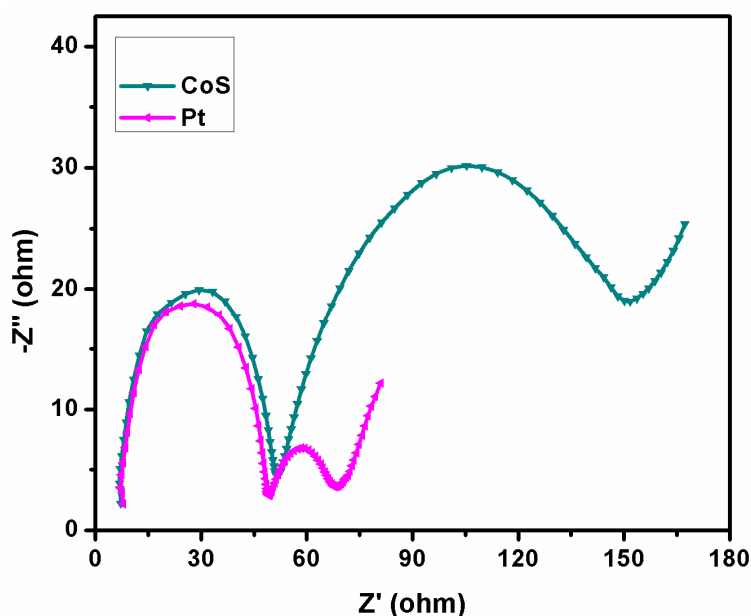
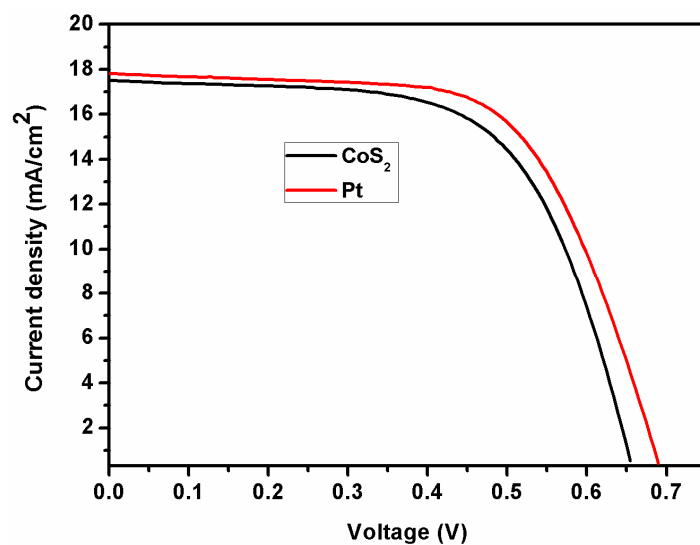


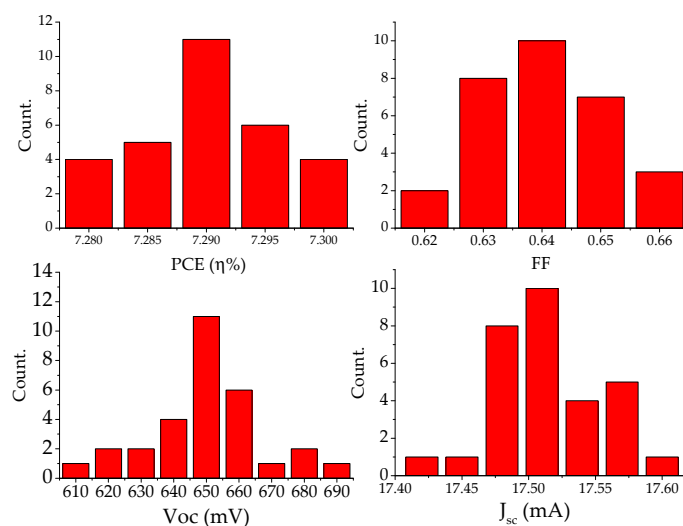
Figure 5. Nyquist plots of EIS for the CoS_2 and Pt CEs.

2.5. Photovoltaic Performance of the DSSCs

Photovoltaic features of the assembled DSSCs [FTO/ $TiO_2:N_3$ /gel-polymer electrolyte/sheet-like CoS_2 /FTO] under an illumination of 1 sun intensity 100 mW/cm^2 (AM 1.5) was investigated. The resulting $J-V$ curves of the DSSCs are displayed in Figure 6a, and the acquired photovoltaic factors comprising short-circuit current density (J_{sc}), open-circuit voltage (V_{oc}), FF, and PCE (η) are listed in Table 1. The fabricated DSSCs have a PCE of 7.29% with an FF of 0.64, V_{oc} of 0.65 V, and J_{sc} of 17.51 mA/cm^2 , which is equivalent to the conventional Pt CE (η of 7.82%). The high PCE of the sheet-like CoS_2 CE is mostly due to its enhanced FF and J_{sc} values, which can be attributed to abundant active electrocatalytic sites and enhanced interfacial charge-transfer by the well-organized surface structure of the CoS_2 CE. The stability test of the DSSCs fabricated using sheet-like CoS_2 and Pt CEs was performed. The DSSCs fabricated with the sheet-like CoS_2 CE retained approximately 82% of its original performance over seven days, whereas the DSSC with the Pt CE retained approximately 90% of its original performance over the same period. This indicates that the stability of the sheet-like CoS_2 CE was analogous to that of the standard Pt CE, and have the potential to be engaged as low cost replacements for Pt CEs in the construction of highly efficient and stable DSSCs. Figure 6b, show the distribution of device performance for 30 devices are shown as a histogram [20,37,38].



(a)



(b)

Figure 6. (a) J - V curves of the DSSCs fabricated with a phthaloylchitosan-based gel-polymer electrolyte using CoS_2 and Pt CEs; (b) the histogram distribution of device parameters such as PCE, J_{sc} , FF and V_{oc} for 30 solar cell test under above said operational parameters.

Table 1. Photovoltaic parameters of the DSSCs fabricated with phthaloylchitosan-based gel-polymer electrolyte using CoS_2 and Pt CEs.

CE	V_{oc} (V)	J_{sc} (mA/cm^2)	FF	η (%)
CoS_2	0.65 ± 0.04	17.51 ± 0.07	0.64 ± 0.02	7.29 ± 0.01
Pt	0.69 ± 0.03	17.81 ± 0.04	0.63 ± 0.02	7.82 ± 0.01

Schematic illustration of the electron transfer process in the DSSCs assembled with phthaloylchitosan-based gel-polymer electrolyte and a CoS_2 CE is shown in Figure 7. Upon illumination, the N_3 dye molecule is photoexcited and the excited dye molecule transfers its electrons to the conduction band (CB) of the TiO_2 electrode. Then, the photoexcited dye molecule regenerates its electrons from the redox mediator in the phthaloylchitosan-based gel-polymer electrolyte. Consequently, the oxidized I^-

ions are reduced to I_3^- at the CoS_2 CE. This cycle is facilitated by the constant flow of electrons from the dye-sensitized TiO_2 photoelectrode to the CoS_2 CE via an outer circuit.

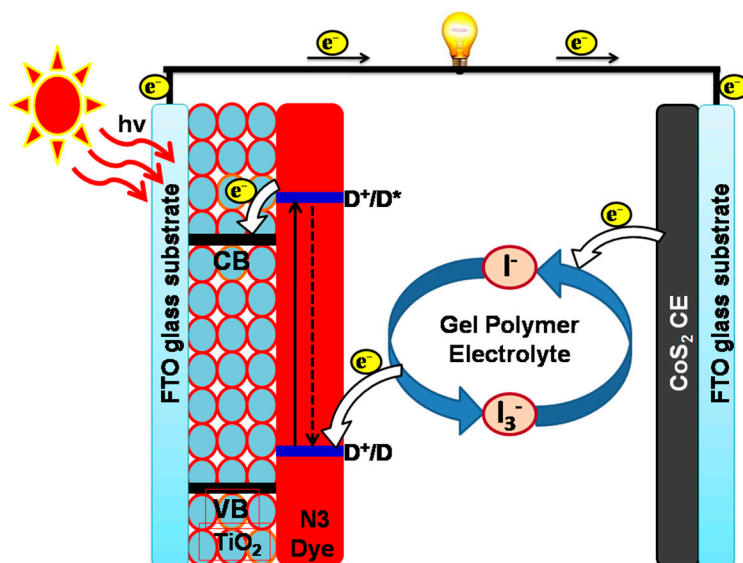


Figure 7. Schematic diagram of the fabricated DSSC based on the CoS_2 CE under illumination.

3. Materials and Methods

3.1. Materials

Acetonitrile, absolute ethanol, thiourea (CH_2CSHCH_2), cobalt (II) chloride hexahydrate ($CoCl_2 \cdot 6H_2O$), ammonia solution (NH_4OH), and iodine (I_2) were purchased from SDFCL (Maharashtra, India). Lithium iodide (LiI), lithium perchlorate ($LiClO_4$), FTO conducting glass (sheet resistance $10 \Omega/cm^2$), and N_3 dye [cis-diisothiocyanato-bis(2,2'-bipyridyl-4,4'-dicarboxylic acid) ruthenium(II)] were acquired from Sigma Aldrich (St Louis, MO, USA). Degussa (Essen, Germany) provided the TiO_2 nanoparticles (P25 and P90). Carbowax was attained from Supelco (Bellefonte, PA, USA). Phthalic anhydride and chitosan were purchased from Merck (Darmstadt, Germany).

3.2. Electrochemical Deposition of the Sheet-Like CoS_2 Films

FTO substrates were washed several times with water and ethanol consecutively and kept in an ultrasonic bath filled with isopropanol for 15 min before deposition. The CoS_2 film was electrodeposited via CV technique with an electrochemical system (CHI608E, CH Instruments, Austin, TX, USA) featuring a three-electrode assembly. The three electrodes were (i) a saturated aqueous $Ag/AgCl$ as a reference electrode; (ii) Pt wire as a CE; and (iii) a precleared FTO as the working electrode. The electrochemical deposition solution was prepared using 0.05 M $CoCl_2 \cdot 6H_2O$ and 1.0 M H_2HCSNH_2 dissolved in 50 mL of water and subjected to magnetic stirring for 15 min. The pH of the electrodeposition solution was maintained at 7.5 by adding ammonia dropwise. The potential range of electrodeposition of the CoS_2 film was from -1.2 to 0.2 V at a scan rate of $5 mVs^{-1}$ for 25 sweep cycles. Lastly, the electrodeposited CoS_2 film was rinsed with water and dried at ordinary temperature.

3.3. Preparation of the Phthaloylchitosan-Based Gel-Polymer Electrolyte

The phthaloylchitosan-based gel-polymer electrolyte was prepared according to previous studies with slight alterations [9]. For instance, a fixed 1.3 wt % poly(ethylene oxide) (PEO, $M_w \sim 5,000,000$), 5.0 wt % phthaloylchitosan, 31.5 wt % dimethylformamide, 22.7 wt % tetrapropylammonium iodide, and 37.8 wt % ethylene carbonate was kept in a closed container and magnetically stirred at $80^\circ C$ for

2 h. After homogeneous gel formation, heating was stopped and the mixture was cooled naturally. Then, 1.7 wt % iodine was added and stirred to obtain a homogeneous phthaloylchitosan-based gel-polymer electrolyte.

3.4. Assembly of the DSSCs

The TiO₂ photoelectrode was prepared in two layers, in which the first was a compact layer prepared by spin coating and the second layer was a porous layer deposited on the first using the doctor blade method. The detailed procedure for the preparation of the TiO₂ photoelectrode was provided in previous reports [12,30]. The TiO₂ coated area on the FTO substrate was coated 0.5 × 0.5 cm and the thickness was around 50 μm. The as-prepared TiO₂ photoelectrode was sensitized by immersion in a 3 mM ethanol solution of N₃ dye for 24 h. The sensitized photoelectrode layer was then rinsed with ethanol solution and dried with hot air. Next, the prepared gel-polymer electrolyte (phthaloylchitosan) was spread uniformly on top of the dye-sensitized TiO₂ layer. Finally, the electrodeposited CoS₂ film CE and prepared dye-sensitized TiO₂ photoelectrode were clamped together to form a sandwich type DSSC. The active device area was 0.2 cm² and photovoltaic investigations were executed in the air atmosphere. The assembled device configuration was FTO/TiO₂/N₃/Gel-polymer electrolyte/CoS₂/FTO. The flow chart for the fabrication of the DSSC device is shown in Figure 8.

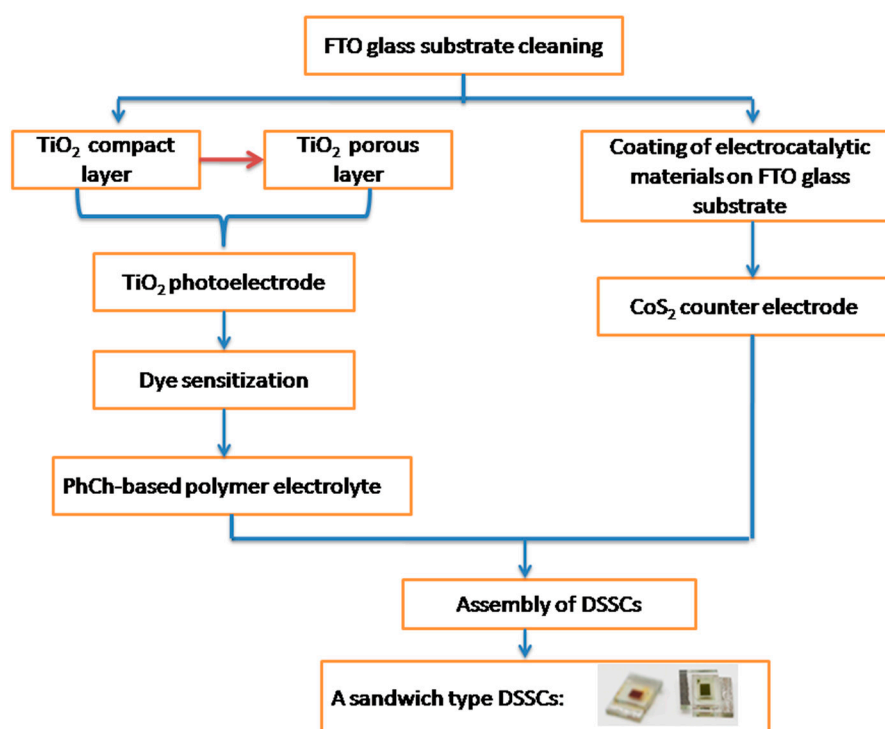


Figure 8. Flowchart describing the fabrication of the DSSCs.

3.5. Characterization Techniques

An X-ray diffractometer (Mini Flex II, Rigaku, The Woodlands, TX, USA) with irradiation of Cu K α ($\lambda = 0.154$ nm) at a scan rate of 4° / min was used to analyze the XRD pattern of the electrochemically deposited CoS₂ thin film. High-resolution scanning electron microscopy (HRSEM) (Quanta FEG 200) with a voltage of 20 kV was used to determine the structural morphology of the fabricated CoS₂ thin film. The HRSEM was also equipped with EDS, which was utilized to define the elemental composition of the film. A tri-electrode (triode) system with Pt-wire as the CE, Ag/AgCl (non-aqueous) as the reference electrode and sheet-like CoS₂ film as the working electrode was used to measure the CV in

100 mM LiClO₄, 1 mM I₂, and 10 mM LiI in acetonitrile. To maintain an inert environment, the solution was N₂ purged for 15 min prior to CV analysis, and the CV curves were measured over a voltage range of −0.6 to +1.2 V. The AC-impedance method with a frequency range of 0.1 Hz to 1.0 MHz and the EIS measurements was carried out in an applied bias at 5 mV AC amplitude. A solar simulator PEC-L01 (PECCELL Inc., Yokohama, Japan) was engaged to investigate photocurrent density-voltage (*J*-*V*) curves of the fabricated DSSCs under 1 sun (100 mW·cm^{−2}) irradiation. The FF and PCE of the fabricated DSSCs with CoS₂ CE in a phthaloylchitosan-based gel-polymer electrolyte were determined with the methods detailed in previous reports [1,6].

4. Conclusions

In summary, a hierarchical sheet-like structured CoS₂ thin film was electrochemically deposited onto an FTO substrate via a simple CV technique. The resulting device was examined using various characterization methods including XRD, HRSEM, and EDS analysis, which revealed the structural properties, surface morphology, and elemental composition of the as-deposited CoS₂ film. CV and EIS analyses indicated improved electrocatalytic behavior of the sheet-like structured CoS₂ thin film for the reduction of I₃[−] to I[−] ions and low *R*_{ct} at the boundary of the CoS₂ CE/electrolyte. Subsequently, the as-deposited sheet-like CoS₂ film was used as a cost-effective and highly efficient Pt-free CE for the fabrication of DSSCs. A phthaloylchitosan-based gel-polymer electrolyte was used as a redox electrolyte for the fabrication of stable DSSCs. The fabricated DSSCs with phthaloylchitosan-based gel-polymer electrolyte and sheet-like CoS₂ CE exhibited an overall PCE of 7.29%, which was comparable to that of conventional Pt CE-based DSSCs (7.20%). The sheet-like structured CoS₂ thin film showed high electrocatalytic activity for the I[−]/I₃[−] redox reaction, which was attributed to abundant active electrocatalytic sites and improved interfacial charge transfer by the well-organized surface structure of the CoS₂ CE. These results indicated that the sheet-like CoS₂ film and phthaloylchitosan-based gel-polymer electrolyte could be used to solve the challenge of fabricating highly efficient, low-cost, and stable DSSCs.

Acknowledgments: The authors are grateful to the Deanship of Scientific Research, King Saud University for funding through Vice Deanship of Scientific Research Chairs.

Author Contributions: This work was performed in collaboration between all authors. The idea was proposed by Saradh Prasad who was responsible for writing the draft of the manuscript. Saradh Prasad, Prabhakarn Arunachalam, and Jayaraman Theerthagiri performed the experimental work, analysis, and discussion of the results. Mohamad Saleh AlSalhi and Govindarajan Durai reviewed the existing literature and placed the research objectives in perspective. Devaraj Durairaj guided and worked in the electrical characterizations, analysis and discussion. All authors managed the reading, editing, and approved the final manuscript.

Conflicts of Interest: The authors declare no conflict of interest.

References

1. Theerthagiri, J.; Senthil, A.R.; Madhavan, J.; Maiyalagan, T. Recent progress in non-platinum counter electrode materials for dye-sensitized solar cells. *ChemElectroChem* **2015**, *2*, 928–945. [[CrossRef](#)]
2. Li, M.H.; Yum, J.H.; Moon, S.J.; Chen, P. Inorganic p-type semiconductors: Their applications and progress in dye-sensitized solar cells and perovskite solar cells. *Energies* **2016**, *9*, 331. [[CrossRef](#)]
3. Schnabel, T.; Seboui, M.; Ahlswede, E. Band gap tuning of Cu₂ZnGeS_xSe_{4−x} absorbers for thin-film solar cells. *Energies* **2017**, *10*, 1813. [[CrossRef](#)]
4. Gratzel, M. Dye-sensitized solar cells. *J. Photochem. Photobiol. C Photochem. Rev.* **2003**, *4*, 145–153. [[CrossRef](#)]
5. Khan, M.Z.H.; Al-Mamun, M.R.; Halder, P.K.; Aziz, M.A. Performance improvement of modified dye-sensitized solar cells. *Renew. Sustain. Energ. Rev.* **2017**, *71*, 602–661. [[CrossRef](#)]
6. Hagfeldt, A.; Boschloo, G.; Sun, L.; Kloo, L.; Pettersson, H. Dye-sensitized solar cells. *Chem. Rev.* **2010**, *110*, 6595–6663. [[CrossRef](#)] [[PubMed](#)]
7. Oliva, D.; Ewees, A.A.; el Aziz, M.A.; Hassanien, A.E.; Cisneros, M.P. A chaotic improved artificial bee colony for parameter estimation of photovoltaic cells. *Energies* **2017**, *10*, 865. [[CrossRef](#)]

8. Bella, F.; Galliano, S.; Gerbaldi, C.; Viscardi, G. Cobalt-based electrolytes for dye-sensitized solar cells: Recent advances towards stable devices. *Energies* **2016**, *9*, 384. [[CrossRef](#)]
9. Theerthagiri, J.; Senthil, R.A.; Buraidah, M.H.; Raghavender, M.; Madhavan, J.; Arof, A.K. Synthesis and characterization of $(\text{Ni}_{1-x}\text{Co}_x)\text{Se}_2$ based ternary selenides as electrocatalyst for triiodide reduction in dye-sensitized solar cells. *J. Solid State Chem.* **2016**, *238*, 113–120. [[CrossRef](#)]
10. Theerthagiri, J.; Senthil, R.A.; Buraidah, M.H.; Madhavan, J.; Arof, A.K. Synthesis of $\alpha\text{-Mo}_2\text{C}$ by carburization of $\alpha\text{-MoO}_3$ nanowires and its electrocatalytic activity towards tri-iodide reduction for dye-sensitized solar cells. *J. Mater. Sci. Technol.* **2016**, *32*, 1339–1344. [[CrossRef](#)]
11. Chen, M.; Shao, L.L. Review on the recent progress of carbon counter electrodes for dye-sensitized solar cells. *Chem. Eng. J.* **2016**, *304*, 629–645. [[CrossRef](#)]
12. Theerthagiri, J.; Senthil, R.A.; Buraidah, M.H.; Bhabu, K.A.; Madhavan, J.; Arof, A.K. Electrochemical deposition of carbon materials incorporated nickel sulfide composite as counter electrode for dye-sensitized solar cells. *Ionics* **2017**, *23*, 1017–1025. [[CrossRef](#)]
13. Theerthagiri, J.; Senthil, R.A.; Buraidah, M.H.; Madhavan, J.; Arof, A.K. Muthupandian Ashokkumar, One-step electrochemical deposition of $\text{Ni}_{1-x}\text{Mo}_x\text{S}$ ternary sulfides as an efficient counter electrode for dye-sensitized solar cells. *J. Mater. Chem. A* **2016**, *4*, 16119–16127. [[CrossRef](#)]
14. Theerthagiri, J.; Senthil, R.A.; Buraidah, M.H.; Madhavan, J.; Arof, A.K. Studies of solvent effect on the conductivity of 2-mercaptopyridine-doped solid polymer blend electrolytes and its application in dye-sensitized solar cells. *J. Appl. Polym. Sci.* **2015**, *132*. [[CrossRef](#)]
15. Theerthagiri, J.; Senthil, R.A.; Buraidah, M.H.; Madhavan, J.; Arof, A.K. Effect of tetrabutylammonium iodide content on PVDF-PMMA polymer blend electrolytes for dye-sensitized solar cells. *Ionics* **2015**, *21*, 2889–2896. [[CrossRef](#)]
16. Senthil, R.A.; Theerthagiri, J.; Madhavan, J.; Murugan, K.; Arunachalam, P.; Arof, A.K. Enhanced performance of dye-sensitized solar cells based on organic dopant incorporated PVDF-HFP/PEO polymer blend electrolyte with $\text{g-C}_3\text{N}_4/\text{TiO}_2$ photoanode. *J. Solid State Chem.* **2016**, *242*, 199–206. [[CrossRef](#)]
17. Senthil, R.A.; Theerthagiri, J.; Madhavan, J.; Arof, A.K. Performance characteristics of guanine incorporated PVDF-HFP/PEO polymer blend electrolytes with binary iodide salts for dye-sensitized solar cells. *Opt. Mater.* **2016**, *58*, 357–364. [[CrossRef](#)]
18. Senthil, R.A.; Theerthagiri, J.; Madhavan, J. Organic dopant added polyvinylidene fluoride based solid polymer electrolytes for dye sensitized solar cells. *J. Phys. Chem. Solids* **2016**, *89*, 78–83. [[CrossRef](#)]
19. Sagaidak, I.; Huertas, G.; Nhien, A.N.V.; Sauvage, F. Towards renewable iodide sources for electrolytes in dye-sensitized solar cells. *Energies* **2016**, *9*, 241. [[CrossRef](#)]
20. Elbohy, H.; Kim, M.R.; Dubey, A.; Reza, K.M.; Ma, D.; Zai, J.; Qian, X.; Qiao, Q. Incorporation of plasmonic au nanostars into photoanodes for high efficiency dye-sensitized solar cells. *J. Mater. Chem. A* **2016**, *4*, 545–551. [[CrossRef](#)]
21. Janani, M.; Srikrishnarka, P.; Nair, S.V.; Nair, A.S. An in-depth review on the role of carbon nanostructures in dye-sensitized solar cells. *J. Mater. Chem. A* **2015**, *3*, 17914–17938. [[CrossRef](#)]
22. Zhao, J.; Ma, J.; Nan, X.; Tang, B. Application of non-covalent functionalized carbon nanotubes for the counter electrode of dye-sensitized solar cells. *Org. Electron.* **2016**, *30*, 52–59. [[CrossRef](#)]
23. Motlagh, M.S.; Mottaghitala, V. The charge transport characterization of the polyaniline coated carbon fabric as a novel textile based counter electrode for flexible dye-sensitized solar cell. *Electrochim. Acta* **2017**, *249*, 308–317. [[CrossRef](#)]
24. Hu, Z.; Xia, K.; Zhang, J.; Hu, Z.; Zhu, Y. Highly transparent ultrathin metal sulfide films as efficient counter electrodes for bifacial dye-sensitized solar cells. *Electrochim. Acta* **2015**, *170*, 39–47. [[CrossRef](#)]
25. Liu, J.; Li, C.; Zhao, Y.; Wei, A.; Liu, Z. Synthesis of NiCo_2S_4 nanowire arrays through ion exchange reaction and their application in Pt-free counter-electrode. *Mater. Lett.* **2016**, *166*, 154–157. [[CrossRef](#)]
26. Yanga, P.; Tang, Q. Bifacial quasi-solid-state dye-sensitized solar cells with metal selenide counter electrodes. *Electrochim. Acta* **2016**, *188*, 560–565. [[CrossRef](#)]
27. Theerthagiri, J.; Senthil, R.A.; Buraidah, M.H.; Madhavan, J.; Arof, A.K. Synthesis of W, Nb and Ta doped $\alpha\text{-Mo}_2\text{C}$ and their application as counter electrode in dye-sensitized solar cells. *Mater. Today Proc.* **2016**, *3*, S65–S72. [[CrossRef](#)]
28. Li, G.R.; Song, J.; Pan, G.L.; Gao, X.P. Highly Pt-like electrocatalytic activity of transition metal nitrides for dye-sensitized solar cells. *Energy Environ. Sci.* **2011**, *4*, 1680–1683. [[CrossRef](#)]

29. Huo, J.; Wu, J.; Zheng, M.; Tu, Y.; Lan, Z. Flower-like nickel cobalt sulfide microspheres modified with nickel sulfide as Pt-free counter electrode for dye-sensitized solar cells. *J. Power Sources* **2016**, *304*, 266–272. [[CrossRef](#)]
30. Sun, H.; Qin, D.; Huang, S.; Guo, X.; Li, D.; Luo, Y.; Meng, Q. Dye-sensitized solar cells with NiS counter electrodes electrodeposited by a potential reversal technique. *Energy Environ. Sci.* **2011**, *4*, 2630–2637. [[CrossRef](#)]
31. Theerthagiri, J.; Senthil, R.A.; Arunachalam, P.; Buraidah, M.H.; Madhavan, J.; Amutha, S.; Arof, A.K. Synthesis of various carbon incorporated flower-like MoS₂ microspheres as counter electrode for dye-sensitized solar cells. *J. Solid State Electrochem.* **2017**, *21*, 581–590. [[CrossRef](#)]
32. Sun, L.; Lu, L.; Bai, Y.; Sun, K. Three-dimensional porous reduced graphene oxide/sphere-like CoS hierarchical architecture composite as efficient counter electrodes for dye-sensitized solar cells. *J. Alloys Compd.* **2016**, *654*, 196–201. [[CrossRef](#)]
33. Bu, I.Y.Y. Sol-gel derived cobalt sulphide as an economical counter electrode material for dye sensitized solar cells. *Optik Int. J. Light Electron. Opt.* **2016**, *127*, 7602–7610. [[CrossRef](#)]
34. Chae, S.Y.; Hwang, Y.J.; Choi, J.H.; Joo, O.S. Cobalt sulfide thin films for counter electrodes of dye-sensitized solar cells with cobalt complex based electrolytes. *Electrochim. Acta* **2013**, *114*, 745–749. [[CrossRef](#)]
35. Sigdel, S.; Dubey, A.; Elbohy, H.; Aboagye, A.; Galipeau, D.; Zhang, L.; Fong, H.; Qiao, Q. Dye-sensitized solar cells based on spray-coated carbon nanofiber/tio₂ nanoparticle composite counter electrodes. *J. Mater. Chem. A* **2014**, *2*, 11448–11453. [[CrossRef](#)]
36. Ma, X.; Elbohy, H.; Sigdel, S.; Lai, C.; Qiao, Q.; Fong, H. Electrospun carbon nano-felt derived from alkali lignin for cost-effective counter electrodes of dye-sensitized solar cells. *RSC Adv.* **2016**, *6*, 11481–11487. [[CrossRef](#)]
37. Li, Y.; Ye, S.; Sun, W.; Yan, W.; Li, Y.; Bian, Z.; Liu, Z.; Wang, S.; Huang, C. Hole-conductor-free planar perovskite solar cells with 16.0% efficiency. *J. Mater. Chem. A* **2015**, *3*, 18389–18394. [[CrossRef](#)]
38. Mallam, V.; Elbohy, H.; Qiao, Q.; Logue, B.A. Investigation of novel anthracene-bridged carbazoles as sensitizers and co-sensitizers for dye-sensitized solar cells. *Int. J. Energy Res.* **2015**, *39*, 1335–1344. [[CrossRef](#)]



© 2018 by the authors. Licensee MDPI, Basel, Switzerland. This article is an open access article distributed under the terms and conditions of the Creative Commons Attribution (CC BY) license (<http://creativecommons.org/licenses/by/4.0/>).